Available online at www.sciencedirect.com

SciVerse ScienceDirect

Ceramics International 39 (2013) 1327–1333

CERAMICS INTERNATIONAL

www.elsevier.com/locate/ceramint

Piezoelectric properties of highly densified 0.01Pb ($Mg_{1/2}W_{1/2}$)O_3–0.41Pb ($Ni_{1/3}Nb_{2/3}$)O_3–0.35$PbTiO_3$–0.23$PbZrO_3$+0.1 wt% Y_2O_3+1.5 wt% ZnO thick films on alumina substrate

Tae Hee Shin[a,b], Jong-Yoon Ha[c], Hyun-Cheol Song[a], Seok-Jin Yoon[a], Hyung-Ho Park[b], Ji-Won Choi[a,*]

[a]*Electronic Materials Research Center, Korea Institute of Science & Technology, Seoul 136-791, Republic of Korea*
[b]*School of Advanced Materials Engineering, Yonsei University, Seoul 120-749, Republic of Korea*
[c]*Institute for Research in Electronics and Applied Physics, University of Maryland, Colleage Park, MD 20742, USA*

Received 7 May 2012; received in revised form 20 July 2012; accepted 20 July 2012
Available online 27 July 2012

Abstract

This paper reports on the formation of highly densified piezoelectric thick films of 0.01Pb($Mg_{1/2}W_{1/2}$)O_3–0.41Pb($Ni_{1/3}Nb_{2/3}$)O_3–0.35$PbTiO_3$–0.23$PbZrO_3$+0.1 wt% Y_2O_3+1.5 wt% ZnO (PMW–PNN–PT–PZ+YZ) on alumina substrate by the screen-printing method. To increase the packing density of powder in screen-printing paste, attrition milled nano-scale powder was mixed with ball milled micro-scale powder, while the particle size distribution was properly controlled. Furthermore, the cold isostatic pressing process was used to improve the green density of the piezoelectric thick films. As a result of these processes, the PMW–PNN–PT–PZ+YZ thick film, sintered at 890 °C for 2 h, showed enhanced piezoelectric properties such as P_r=42 μC/cm^2, E_c=25 kV/cm, and d_{33}=100 pC/N, in comparison with other reports. Such prominent piezoelectric properties of PMW–PNN–PT–PZ+YZ thick films using bi-modal particle distribution and the CIP process can be applied to functional thick films in MEMS applications such as micro actuators and sensors.

Keywords: Piezoelectric thick film; Screen-printing; Particle size control; Cold isostatic pressing

1. Introduction

Lead zirconium titanate (PZT) has been widely used in various electric components, such as sensors, actuators, and filters, because of its excellent properties including high force generation, quick response time, low power consumption and large displacement. Piezoelectric thick films are of extreme interest in recent decades due to the miniaturization of devices and, particularly, the development of micro electromechanical system (MEMS) technology. Piezoelectric thick films are required for the essential function of sensing and actuating in MEMS devices such as micropumps, micro fluidic devices, accelerometers, ultrasonic transducers, ultrasonic devices, ink-jet printer heads, microactuators for high-density hard-disk drives and bio sensors using cantilever [1–4]. Those MEMS devices require specific thickness of piezoelectric films to obtain their sufficient power and force. For instance, the thickness of the piezoelectric films are in the range of 0.5–5 μm for MEMS application, 2–10 μm for microactuators to generate large force, 30–50 μm for ultrasonic transducers with over 50 MHz frequency, and 100 μm–2 mm for millimeter size devices [4]. The piezoelectric films can be formed using various methods such as sol–gel processing [5,6], sputtering deposition [7], pulsed laser deposition (PLD) [8], chemical vapor deposition (CVD) [9], and screen-printing [10]. Almost all these deposition processes are appropriate for the fabrication of thin films with less than a couple of micron thickness because of their film deposition rates and the internal stress which can generate crack propagations in the films. To form thick films on the substrate using bulk machining and bonding has disadvantages such as expensive cost, and difficulties in both the manufacture of complicated shapes and the handling of ceramics.

*Corresponding author. Tel.: +82 2 958 5556; fax: +82 2 958 6720.
E-mail address: jwchoi@kist.re.kr (J.-W. Choi).

0272-8842/$ - see front matter
http://dx.doi.org/10.1016/j.ceramint.2012.07.068

However, the conventional screen-printing technology fabricates single layer films less than 100 μm with wide areas at a low cost. This unique method for the thick films is competitive, simple, and flexible [11]. However, the screen-printing method causes serious drawbacks such as low density and other lower properties of thick films compared to the properties of bulk. These drawbacks arise because pores in the films are produced during the binder burnout process. Also, the substrate clamping prevents sufficient grain growth and densification of thick films.

In this paper, $0.01Pb(Mg_{1/2}W_{1/2})O_3$–$0.41Pb(Ni_{1/3}Nb_{2/3})O_3$–$0.35PbTiO_3$–$0.23PbZrO_3$+0.1 wt% Y_2O_3+1.5 wt% ZnO (PMW–PNN–PT–PZ+YZ) composition which has good piezoelectric properties [12] with low sintering temperature was chosen for forming films. We have also reported that the optimized mixture condition for two types of particles, ball milled and attrition milled, is 3:1 ratio [13]. That ratio of the particles improves the density and other properties of piezoelectric thick films prepared by screen-printing. To further improve the density of piezoelectric thick films on the alumina substrate, cold isostatic pressing (CIP, Autoclave engineer Co., USA) was conducted before the sintering process.

2. Experimental procedure

The composition of the ceramics used in this study is $0.01Pb(Mg_{1/2}W_{1/2})O_3$–$0.41Pb(Ni_{1/3}Nb_{2/3})O_3$–$0.35PbTiO_3$–$0.23PbZrO_3$+0.1 wt% Y_2O_3+1.5 wt% ZnO. The startng materials are PbO (99.9% Kosudo, Japan), MgO (98% Aldrich, USA), WO_3 (99% Kanto, Japan), NiO (99% Aldrich, USA), Nb_2O_5 (99.9% Aldrich, USA), ZrO_2 (99.9% Aldrich, USA), TiO_2 (99% Aldrich, USA), Y_2O_3 (99.99% Aldrich, USA) and ZnO (99.9% Aldrich, USA).

The stoichiometry PMW–PNN–PT–PZ+YZ ceramics were prepared by a conventional solid solution method. The starting materials were mixed in water for 24 h by ball milling process. The mixtures were dried and then calcined in an alumina crucible at 850 °C for 2 h in air. The calcined powder was milled again with the additives of 0.1 wt% Y_2O_3 and 1.5 wt% ZnO for 48 h. To produce submicron size particles, the dried powder was milled by an attrition milling for 24 h. The 25 wt% of attrition milled powders were mixed with the ball milled powder in order to improve packing density of powders [13]. Average particle sizes and the particle size distributions of the powders were measured using a particle size analyzer (Cilas 1064L, France). The mixture powder and a commercialized binder (B-75001, Ferro Co., USA) blended together to make piezoelectric paste using a three-roll miller. The amount of the vehicle were 20 wt% of the PMW–PNN–PT–PZ+YZ mixture. The bottom silver–palladium (Ag–Pd) electrodes were formed by screen-printing on the alumina substrates and then fired them at 1050 °C for 20 min. The bottom electrodes were 5 μm thick. 25 μm-thick piezoelectric layers were printed on the bottom electrodes. After that, the films were dried at 120 °C for 20 min to evaporate the solvent and then burned out at 450 °C for 2 h to remove the binder. A CIP process was conducted at 30000 psi (2109 kgf/cm^2) for 30 min in order to increase the green density of the piezoelectric layers. The specimens were sintered in the temperature range from 850 °C to 890 °C for 2 h with 5 °C/min of the heating and cooling rates in a box furnace. Pt electrodes as top electrodes were deposited using a DC sputter.

The sintered films were examined by X-ray diffraction (XRD, Model Rint/Dmax 2500, Rigaku, Japan) analysis with Cu–Kα radiation. The microstructures of the piezoelectric ceramics were investigated using a scanning electron microscope (SEM, Model H-3000, Hitachi, Japan). The piezoelectric properties were measured at 1 kHz by a precision impedance analyzer (4294A, Agilent, USA). Corona poling took place at room temperature with a tip-sample distance of 10 cm and an applied voltage of 15 kV. The piezoelectric constants in the films were measured by the Berlincourt method. The polarization–electric field (P–E) hysteresis loops of the films were measured at 1 kHz using a modified Sawyer–Tower circuit.

3. Results and discussion

The packing density of a powder that is mainly determined by powder size distributions can influence the sintered density and other properties of bulk ceramics [14]. In the same way, if the particles for piezoelectric thick films are properly controlled, the physical and electrical properties of the piezoelectric films should be improved. Fig. 1 shows SEM images of prepared powders by various methods such as attrition billed, ball milled, and mixture powders consisting of 75 wt% ball milled and 25 wt% attrition milled powders, and particle size distributions of the mixture powder. Two types of powders which were attrition milled and ball milled powders showed quite different particle sizes and morphologies in Fig. 1(a) and (b). The powder was mixed with 1.51 μm mean diameter of the ball milled powder and 0.26 μm mean diameter of the attrition milled powder. The distribution of the mixture powder showed the typical bi-modal distribution we expected, because two types of particles, such as coarse and fine particles, were mixed together as shown in Fig. 1(c) and (d). From our previous results, which were on PMW–PNN–PT–PZ+YZ thick film on Si substrate without CIP process [13], we know that adding 25 wt% attrition milled powder to the ball milled powder resulted in a maximum packing density. That result showed that the bi-modal distribution generally has higher packing density than mono-modal distribution. The volume fraction of the fine and coarse powder shown in Fig. 1(d) is similar to that shown in the previous result [13]. The total mean size of the mixture powder was 1.18 μm. In 1928, C.C. Furnas [15,16] theoretically calculated that the highest packing density uses large coarse particles and small fine particles together. Furnas showed that the composite packing density is typically highest when $f=0.735$ (f, coarse volume) for the ideal dense packing of bi-modal sphere particles, where the coarse and fine particles were uniform in size, respectively. However,

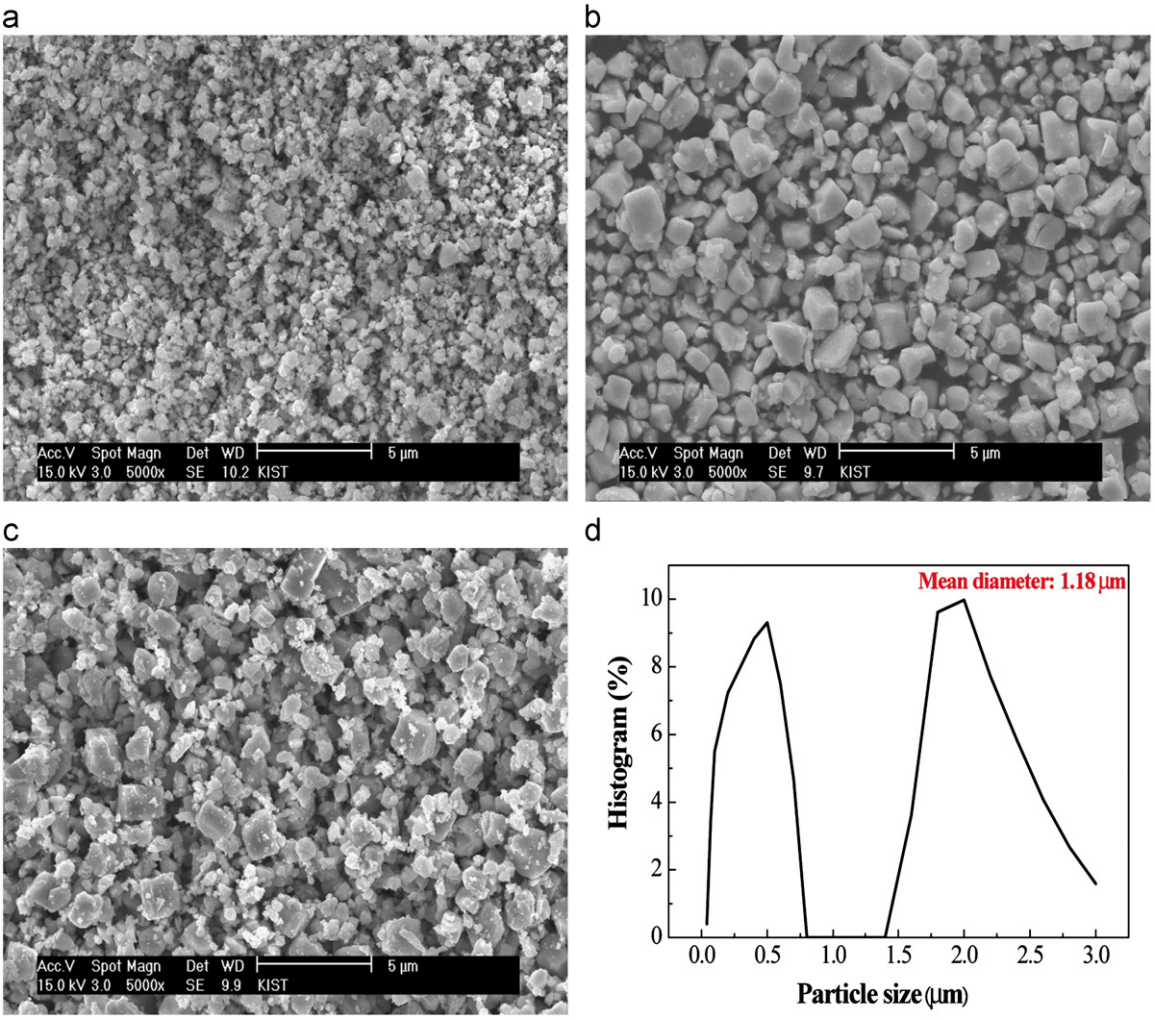

Fig. 1. SEM images of (a) attrition milled powder (b) ball milled power (c) the mixed powder of the attrition and ball milled powders (ball milled powder: attrition milled powder = 3:1) and (d) particle size distribution graphs of the mixed powder of attrition and ball milled powders (ball milled powder: attrition milled powder = 3:1).

in our experiments, the screen-printed thick films fabricated by ball or attrition milled powders were not ideally densified because the particles had multi-sized diameters and were not evenly distributed [17]. As, our previous result [13] showed the f for our compositions was 0.451, under the optimized mixing rate.

Fig. 2 shows the surface morphologies of the as printed and cold-isostatic pressed piezoelectric thick films sintered at the temperature range from 850 to 890 °C for 2 h. First, Fig. 2(a) and (b) show the surface morphologies of the as printed and pressed samples. These images indicated that both films were well formed with the binder on the substrates. After the cold-isostatic pressing, the surface morphology of the film seemed to be slightly improved. The uniform grain sizes of each sample, shown in Fig. 2(c), (d), and (e), were from less than 1 μm to 2 μm, respectively. The porosities of the PMW–PNN–PT–PZ + YZ thick films would be estimated as decreased with increasing sintering temperature due to the increase of grain size, and the thick films sintered at 890 °C showed the densest microstructure of all the films. The grain sizes of the films were very similar to those of our previous results. However, the porosities of the films slightly decreased through the SEM analysis [13,18]. The results implied that the bimodal distributed powder should improve the porosity of the thick films.

Fig. 3 shows X-ray diffraction patterns of the PMW–PNN–PT–PZ + YZ thick films sintered at various temperatures. All peaks of the samples were indexed in terms of the simple cubic perovskite (Pm3) unit cell with pyrochlore phase in all range of the sintering temperature. Generally, the presence of pyrochlore was recognized when the PZT system films were annealed to form the perovskite phase. The intensity of the pyrochlore phase was decreased with increasing sintering temperature. At a higher sintering temperature, more perovskite phase was formed, which meant that almost of the pyrochlore phase transformed to perovskite phase, as shown in Fig. 3(c) [19].

P–E hysteresis loops of piezoelectric thick films sintered at 850 °C, 870 °C and 890 °C for 2 h are shown in Fig. 4.

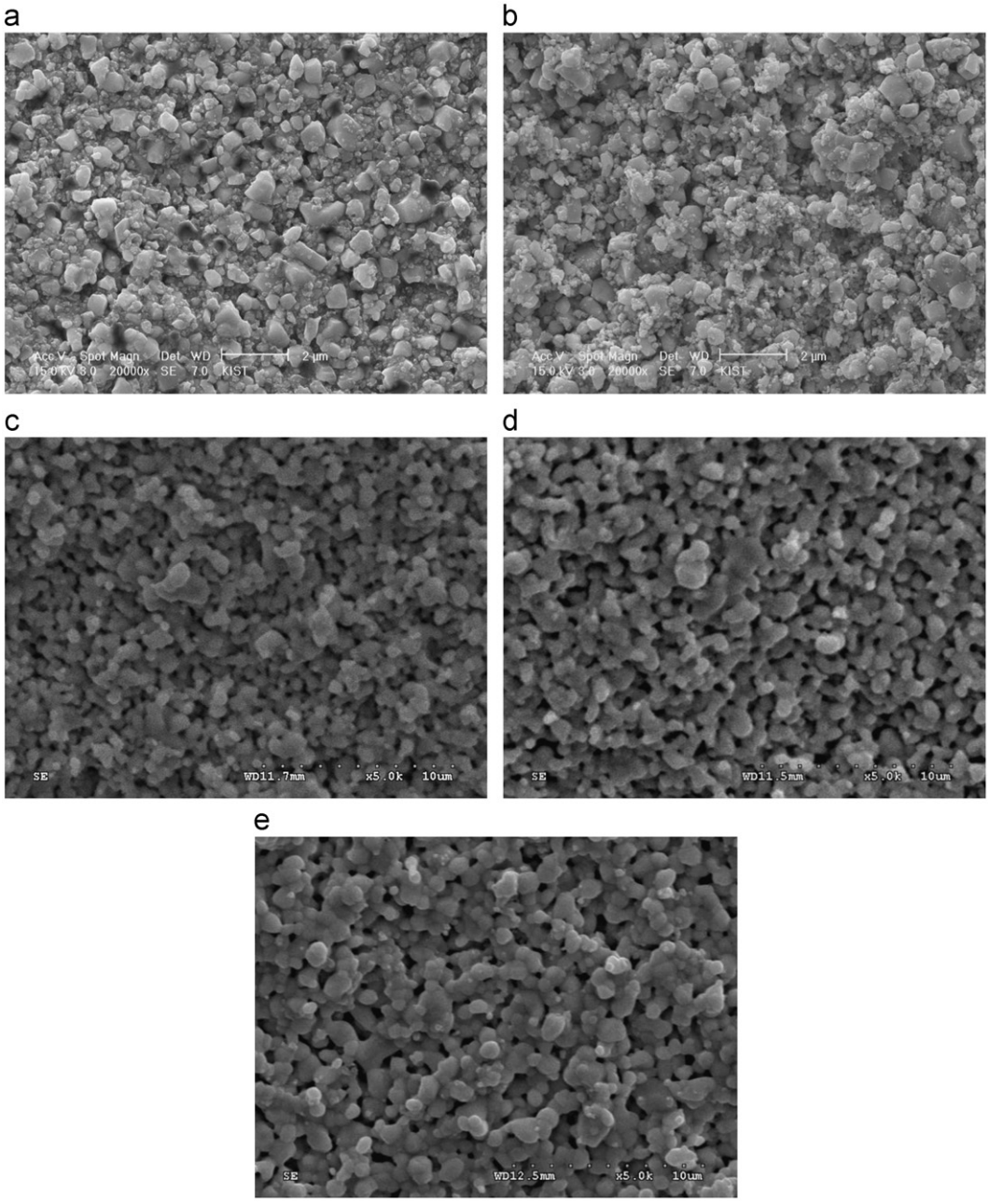

Fig. 2. Surface morphologies of the PMW–PNN–PT–PZ+YZ thick films (a) as printed, (b) cold-isostatic pressed, sintered at (c) 850 °C, (d) 870 °C, and (e) 890 °C on alumina substrates.

The P–E hysteresis loops measured at 1 kHz showed a typical ferroelectric character. The remanent polarizations (P_r) of the piezoelectric thick films were significantly increased with the increase of sintering temperature. A maximum P_r value of 42 μC/cm^2 at 890 °C for 2 h was obtained. The reason why the maximum P_r showed at 890 °C was that the densification of thick films was maximized and the pyrochlore phase was significantly decreased. The value of the P_r at 890 °C was close to values of the bulk PMW–PNN–PT–PZ+YZ compositions [6,12,18]. In addition, the P_r that we developed was one of the higher values (>35 μC/cm^2) ever developed through piezoelectric thick film processes. The coercive field (E_c) at 890 °C for 2 h was 25 kV/cm. These ferroelectric properties of the thick film at 890 °C could be utilized for piezoelectric microactuators and microsensors [20].

Fig. 5 shows dielectric constants and losses of the PMW–PNN–PT–PZ+YZ films measured at 1 kHz with variations of sintering temperatures. The relative dielectric constants increased and the dielectric losses decreased with increasing sintering temperature from 850 to 890 °C for 2 h. Those results could be explained in terms of the densification of thick films and the reduction of the pyrochlore phases in the films. The dielectric constant and the

dielectric loss of the piezoelectric film at 890 °C for 2 h were 2400 and 0.067 at 1 kHz, respectively.

The piezoelectric constant (d_{33}) was measured by the Berlincourt method after the corona poling with a tip-sample distance of 10 cm and an applied voltage of 15 kV. Fig. 6 shows that the d_{33} values were dramatically increased during the increase of the sintering temperature from 850 to 890 °C for 2 h. The maximum d_{33} values of 100 pC/N was obtained at 890 °C. Generally, the d_{33} values of the films on the substrates were conspicuously lower than the values of the bulks because of the clamping of the substrate. Even though some papers [10,21,22] have reported about the d_{33} value, those were still around 50 pC/N. The d_{33} value of the PMW–PNN–PT–PZ+YZ thick film sintered at 890 °C for 2 h was higher than in other published results because the amount of pyrophase and porosity of the thick films was significantly decreased, as shown in XRD patterns and SEM images.

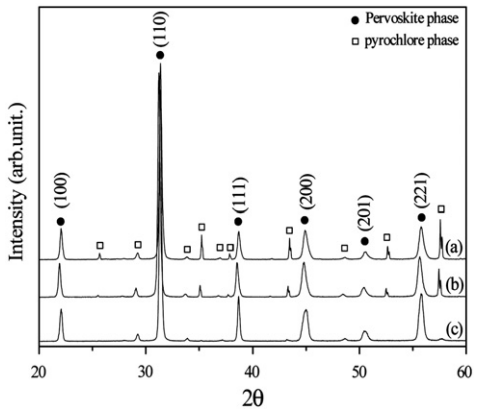

Fig. 3. X-ray diffraction patterns of the PMW–PNN–PT–PZ+YZ thick films sintered at (a) 850 °C, (b) 870 °C, and (c) 890 °C on alumina substrates.

4. Conclusions

This paper has demonstrated the formation of a highly densified piezoelectric thick film by the screen-printing method. The mixture of PMW–PNN–PT–PZ+YZ ceramics consisting of 75 wt% micro and 25 wt% nano size powers had the highest packing density. Furthermore, the CIP process improved the green density of the piezoelectric thick films. The PMW–PNN–PT–PZ+YZ thick film sintered at 890 °C showed tremendous piezoelectric properties such as P_r=42 μC/cm^2, E_c=25 kV/cm, and d_{33}=100 pC/N, in comparison with the previous reports. Those prominent piezoelectric properties of PMW–PNN–PT–PZ+YZ thick films using bi-modal particle distribution

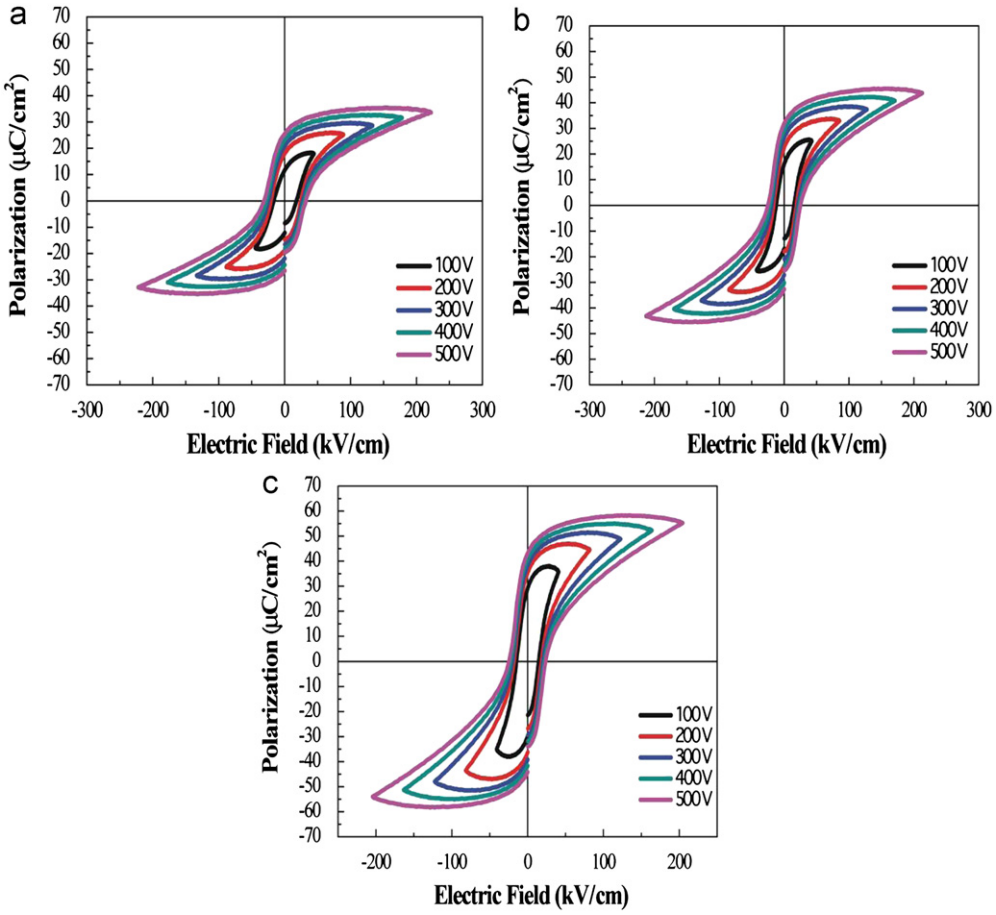

Fig. 4. P–E hysteresis loops of the PMW–PNN–PT–PZ+YZ thick films sintered at (a) 850 °C, (b) 870 °C, and (c) 890 °C on alumina substrates.

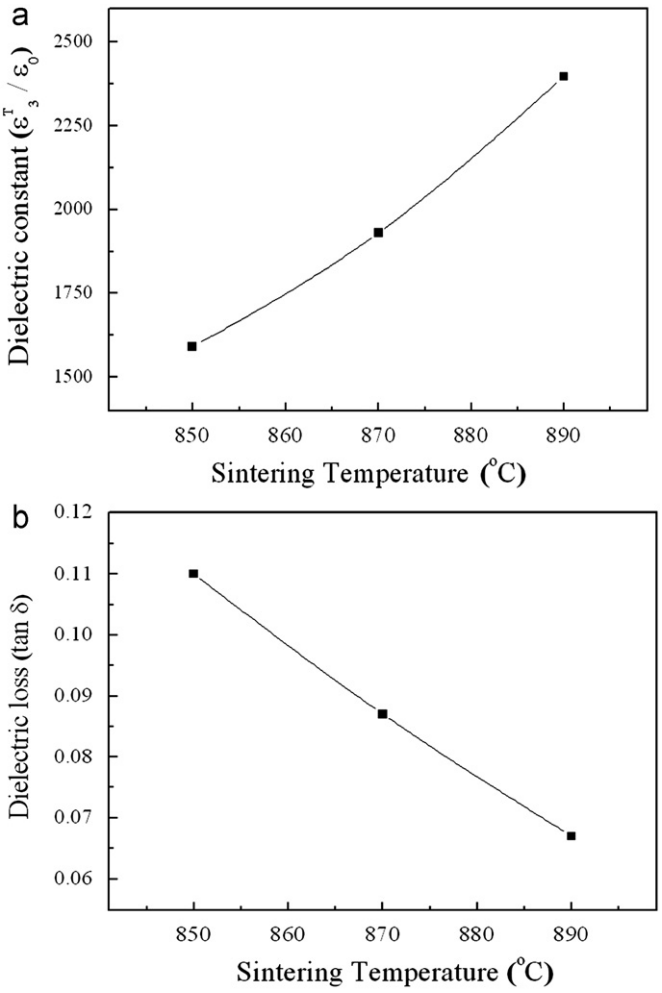

Fig. 5. (a) Dielectric constants and (b) losses of the PMW–PNN–PT–PZ+YZ thick films measured at 1 kHz with various sintering temperatures.

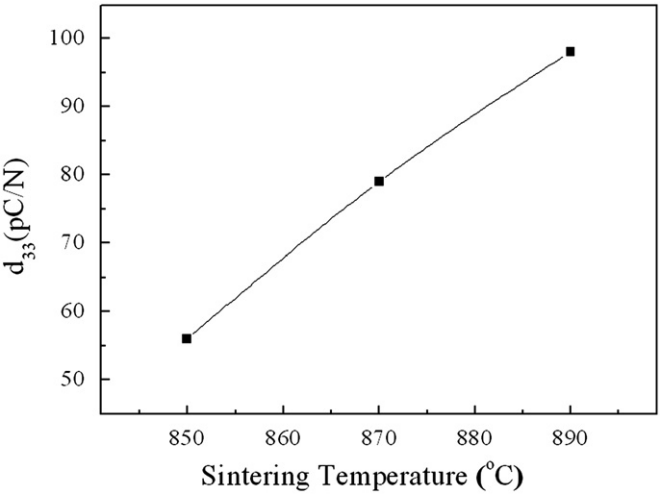

Fig. 6. Piezoelectric constants of the PMW–PNN–PT–PZ+YZ thick films with various sintering temperatures.

and the CIP process are applicable for functional thick films in MEMS applications such as micro actuators and sensors.

Acknowledgments

This work was financially supported by the 21st Century's Frontier R & D program and KIST Future Resource Program.

References

[1] E.-H. Yang, Y. Hishinuma, J.-G. Cheng, S. Trolier-Mckinstry, E. Bloemhof, B.M. Levine, Thin-film piezoelectric unimorph actuator-based deformable mirror with a transferred silicon membrane, Journal of Microelectromechanical Systems 15 (2006) 1214–1225.

[2] P. Muralt, A. Kholkin, M. Kohli, T. Maeder, Piezoelectric actuation of PZT thin-film diaphragms at static and resonant conditions, Sensors and Actuators A 53 (1996) 398–404.

[3] J.H. Lee, K.H. Yoon, K.S. Hwang, J. Park, S. Ahn, T.S. Kim, Label free novel electrical detection using micromachined PZT monolithic thin film cantilever for the detection of C-reactive protein, Biosensors and Bioelectronics 20 (2004) 269–275.

[4] N. Ledermann, P. Muralt, J. Baborowski, M. Forster, J.P. Pellaux, Piezoelectric $Pb(Zr_x,Ti_{1-x})O_3$ thin film cantilever and bridge acoustic sensors for miniaturized photoacoustic gas detectors, The Journal of Micromechanics and Microengineering 14 (2004) 1650–1658.

[5] Z. Wang, W. Zhu, C. Zhao, O.K. Tan, P.Z.T. Dense, Thick Films derived from sol–gel based nanocomposite process, Materials Science and Engineering B 99 (2003) 56–62.

[6] Z.-X. Zhu, J.-F. Li, F.-P. Lai, Y. Zhen, Y.-H. Lin, C.-W. Nan, L. Li, Phase structure of epitaxial $Pb(Zr,Ti)O_3$ thin films on Nb-doped $SrTiO_3$ substrates, Applied Physics Letters 91 (2007) 222910.

[7] C. Wang, Q.F. Fang, Z.G. Zhu, A.Q. Jiang, S.Y. Wang, B.L. Cheng, Z.H. Chen, Dielectric properties of $Pb(Zr_{20}Ti_{80})O_3/Pb(Zr_{80}Ti_{20})O_3$ multilayered thin films prepared by RF magnetron sputtering, Applied Physics Letters 82 (2003) 2880–2882.

[8] S.S. Kim, B.I. Kim, Y.B. Park, T.S. Kang, J.H. Je, Growth of a textured $Pb(Zr_{0.4}Ti_{0.6})O_3$ thin film on $LaNiO_3$/Si(001) using pulsed laser deposition, Applied Surface Science 169–170 (2001) 553–556.

[9] C.H. Lin, P.A. Friddle, C.H. Ma, A. Dag, H. Chen, Effects of thickness on the electrical properties of metal organic chemical vapor deposited $Pb(Zr,Ti)O_3$ (25–100 nm) thin films on $LaNiO_3$ buffered Si, Journal of Applied Physics 90 (2001) 1509–1511.

[10] R.N. Torah, S.P. Beeby, M.J. Tudor, N.M. White, Thick-film piezoceramics and devices, Journal of Electroceramics 19 (2007) 95–110.

[11] V. Walter, P. Delobelle, P. Le Moal, E. Joshph, M. Collet, A Piezomechanical characterization of PZT thick films screen-printed on alumina substrate, Sensors and Actuators A 96 (2002) 157–166.

[12] S.-J. Kim, C.-Y. Kang, J.-W. Choi, H.-J. Kim, M.-Y. Sung, S.-J. Yoon, Low temperature sintering of ZnO-doped 0.01Pb-$(Mg_{1/2}W_{1/2})O_3$–0.41Pb$(Ni_{1/3}Nb_{2/3})O_3$–0.35$PbTiO_3$–0.23$PbZrO_3$ ceramics, Japanese Journal of Applied Physics 46 (2007) 276–279.

[13] H.-G. Moon, H.-C. Song, S.-J. Kim, J.-W. Choi, C.-Y. Kang, S.-J. Yoon, Piezoelectric properties and microstructure of 0.01Pb$(Mg_{1/2}W_{1/2})O_3$–0.41Pb$(Ni_{1/3}Nb_{2/3})O_3$–0.35$PbTiO_3$–0.23$PbZrO_3$ thick film with particle size distribution, Journal of the Korean Physical Society 17 (2008) 418–424.

[14] S. Taruta, K. Kitajima, N. Takusagwa, K. Okada, N. Otsuka, Influence of coarse particle size on packing and sintering behavior of bimodal size distributed alumina powder mixtures, Journal of the Ceramic Society of Japan 101 (1993) 583–588.

[15] C.C. Furnas, Department of Commerce, Bureau of Mines, Report of Investigation Serial No. 2894, 1928; Bulletin of US Bureau of Mines 307, 74 (1929).

[16] C.C. Furnas, Grading aggregates: I – mathematical relations for beds of broken solids of maximum density, Industrial and Engineering Chemistry 23 (1931) 1052–1058.

[17] D.C.C. Lam, M. Nakagawa, Packing of particles (Part 3), Journal of the Ceramic Society of Japan 102 (1994) 133–138.

[18] S.-J. Kim, C.-Y. Kang, J.-W. Choi, H.-J. Kim, M.-Y. Sung, S.-J. Yoon, Characteristics of PMW–PNN–PT–PZ thick films on various bottom electrodes, Journal of Electroceramics 17 (2006) 495–498.
[19] C.K. Kwok, S.B. Desu, Pyrochlore to perovskite phase transformation in sol–gel derived lead–zirconate–titanate thin films, Applied Physics Letters 60 (1992) 1430–1432.
[20] B.Y. Lee, C.I. Cheon, J.S. Kim, K.S. Bang, J.C. Kim, H.G. Lee, Low temperature firing of PZT thick films prepared by screen printing method, Materials Letters 56 (2002) 518–521.
[21] R.A. Dorey, R.W. Whatmore, Apparent reduction in the value of the d_{33} piezoelectric coefficient in PZT thick films, Integrated Ferroelectrics 50 (2002) 111–119.
[22] R.N. Torah, S.P. Beeby, M.J. Tudor, N.M. White, Improving the piezoelectric properties of thick-film PZT: the influence of paste composition, powder milling process and electrode material, Sensors and Actuators A 110 (2004) 378–384.